RSC Advances

ROYAL SOCIETY OF CHEMISTRY

www.rsc.org/advances

Cite this: DOI: 10.1039/c0xx00000x

www.rsc.org/xxxxxx

ARTICLE TYPE

Redox-responsive Cystamine Conjugated Chitin-Hyaluronic Acid Composite Nanogels

*N. Ashwinkumar[#], S. Maya[#], R. Jayakumar**

Received (in XXX, XXX) XthXXXXXXXXX 20XX, Accepted Xth XXXXXXXXX 20XX

DOI: 10.1039/b000000x

Nanoscale carriers were developed to overcome the challenging barriers for targeted intracellular delivery of the chemotherapeutic agents specifically within the tumors. We demonstrate redox responsive cystamine (Cys) conjugated Hyaluronic acid (HA)-Chitin (CNG) nanogels for the intracellular delivery of Doxorubicin (DOX) within colon cancer cells. Chitin having a slow degrading property could make HA to degrade slowly thereby protecting DOX from a sudden burst release and also HA being a ligand for CD44 receptor over expressed in colon cancer cells (HT-29). 150-200 nm sized DOX-HA-CNGs and DOX-HA-Cys-CNGs were developed and well characterized with DLS, Zeta, TG/DTA, FT-IR, EDAX and rheological techniques. The composite nanogel preparations proved to be safe for intravenous administration as they were non-hemolytic and did not interfere with the coagulation cascade. Flow cytometric and fluorescent microscopic analysis proved specific internalization of DOX-HA-CNGs within HT-29 cells (CD-44 +ve). MTT assay showed the superior anti-proliferative activity for DOX-HA-Cys-CNGs in CD-44+ve HT-29 cells than that in CD-44 –ve IEC-6 cells. Thus HA-Cys-CNGs proved to be a better carrier for selective, redox responsive and intracellular delivery of DOX.

Introduction

In the field of drug delivery, the attention of the researchers was towards hydrogels due to their innate tunable properties such chemical,[1] physical,[2] thermal[3] and pH.[4] Primarily, these hydrogels from natural polymers were used for tissue engineering applications for tissue damages and replacements.[5,6] The properties of them were tuned, that motivated the research on drug delivery applications.[7] Hydrogels are defined as three-dimensional polymeric networks and they have the capability of imbibing water or biological fluids.[8] Hydrogel containing functional groups such as hydroxyl group, amide group and protonated amine group, have the tendency to absorb and swell with respect to the environmental conditions.[9] These can be linked either by physical or chemical nature through covalent bonding, hydrogen bonding, van-der-waals interactions or physical entanglements.[10] Although hydrogels are very popular, they have certain drawbacks which make the researchers to focus on converting these hydrogels to nanoregime with more specific and attractive properties.[11] Diffusion is the main factor and also the biggest drawback in these hydrogel systems, in which the signal transduction is very less when compared to nanoregime.[12] To overcome these above problems, hydrogels are converted into nanogels, which have increased surface to volume ratio. There might be an increase in diffusion, conjugation with antibodies and drug volume. To induce these signals and to provide more functionality, interconnected pores can be introduced in the polymers by bottom up approach converting hydrogels to nanogels.[13] These three dimensional polymeric scalar matrices were developed by cross linking the polymers called "Nanogels".[14] These nanogels are highly hydrophilic polymers, having an innate swelling property and high drug loading capacity.[15] Since these nanogels were prepared in hydrophilic region, the need for surfactants is minimal. Nanogels are synthesized by various approaches like physical interaction of polymers, interfacial sol-gel, polymerizing the monomers and cross linking the pre-processed polymer.[16] These nanogels have more affinity towards water and hence the mononuclear phagocyte uptake would be minimal.[17] In general, nanogels having high surface to volume ratio helps in modifying the surface by chemically conjugating target moieties for ligand-receptor interaction.[18,19] On the whole, nanogels demonstrate excellent potential for enhancing oral, brain bioavailability and systemic drug delivery of hydrophilic and low molecular weight drugs.[20,21]

Nanogels have been synthesized using various biopolymers and synthetic polymers like chitosan, pullalan,[22] cellulose,[23] poly(lactic-co-glycolic) acid (PLGA),[24] poly ethylene glycol and polycaprolactone (PCL).[25] One of the commonly present biopolymer in our body is in the form of "hyaluronan".[26] Hyaluronan is also called as Hyaluronic acid (HA) which is a bioinert, anionic and non-sulfated glucosaminoglycan with an average molecular weight of 140KDa similar to that of chitin. The presence of hyaluronan in human body maintains the integrity of extracellular matrices. It can also be considered as natural moisturizer, which could be due to the presence of hydrophilic molecules in HA.[27] A special property of HA acting as ligand for CD44 receptor which involves in various mechanism like converting native form of hyaluronan to water, cell migration and cell signaling etc. The degradation of hyaluronic acid would be faster due to the presence of special enzyme called "Hyaluronidases".[28] HA is commonly present in

tissues like skin, tendons and ligaments and helps in the water retention as well as in the tissue coordination and the level of HA should be maintained continuously.[29] Recently, native form of HA is used for the anti-aging property.[26] The major isoform of CD44 is CD44v6,[29] which is over expressed in colon cancer cells, metastatic and non-metastatic tumors.[30] Investigation of human breast cancer proved that the connective tissues having high level of hyaluronic acid in benign stage. So, the presence and requirement of HA in tumor region can be considered to detect malignant tumors and also act as marker for detecting level of cancer growth.[31] Other than Hyaluronic acid, chitin is also a well known biopolymer used for various applications like tissue engineering, drug delivery, and protein delivery. Chitin is similar to HA connected derivative of glucose consisting of N-acetyl glucosamine and highly cationic in nature due to the presence of amine group.[32] When compared to nanogels, composite nanogels showed different perspective towards therapeutic and diagnostic applications. Composite nanogels were completely prepared and optimized with simple chemical cross linking between two polymers. The reduced glutathione (GSH) and oxidized form of glutathione (GSSG) mechanism is always maintained to regulate cells such as cell differentiation, proliferation, and apoptosis.[33] The conjugation of cystamine, which contains the disulphide bond in the molecule, is used in delivering the drug inside the cells. Cystamine can be easily reduced with the help of GSH reducing agent inside the cells for drugs release mechanism.[34,35] In this study, hyaluronic acid (HA) and chitin were used to develop composite nanogels for glutathione based controlled delivery of hydrophilic drug doxorubicin. Cystamine dihydrochloride contains disulphide bond linked between chitin and hyaluronic acid which acts as a reduced glutathione (GSSG). This oxidized form of glutathione (GSSG) gets converted to oxidized glutathione GSH inside the cell in-order to maintain the cellular mechanism and release of drugs would occur in controlled manner. Hyaluronic acid, which acts as a ligand for CD44 receptor in the colon cancer cells, helps in uptake of these composite nanogels.

Experimental Details

(a) Materials

Chitin (degree of acetylation 72.4%, molecular weight 150 KDa) was purchased from Koyo Chemical Co. Ltd., Japan. Hyaluronic acid (MW-140KDa) was purchased from Qingdao Haitao Biochemical Co. Ltd. China, Cystamine dihydrochloride (MW – 225 g/mol) was purchased from Alfa Aesar, India. Reduced Glutathione (MW – 307 g/mol) from Loba Chemi, India, Calcium chloride and methanol was purchased from Qualigens, India and Doxorubicin hydrochloride (Dox) from Pfizer, India. The HT-29 (colon cancer cells) and IEC-6 (intestinal epithelial) cell lines were purchased from NCCS Pune, India. Media (DMEM) for culturing cells was purchased from Sigma Aldrich.

(a) Preparation of DOX loaded Cystamine conjugated Hyaluronic acid/Chitin composite nanogels (DOX-HA-Cys-CNGs):

50 mg of HA was taken and dissolved in 5ml of milliQ water under stirring. 2ml of prepared hyaluronic acid solution was added slowly in a drop wise to α-Chitin solution, which is dissolved in saturated calcium chloride in methanol and stirred overnight resulting in composite gels.[36] These composite gels were processed with several washing steps (centrifugation – 20000rpm, sonication – 75% amplitude) to form HA-CNG composite nanogels. 5mg of Cystamine dihydrochloride ((Cys) dissolved in 1ml of milli-Q water) acts as a cross linker between the Chitin and HA. Firstly, 2mL HA was incubated with 500uL of EDC (5mg/ml) for 3 hr followed by the addition of 500uL of Cys (5mg/ml) and stirred overnight.[26] The above prepared complete solutions were added to 0.5% of chitin solution (5mg/mL) to form a gel like structure. After gel formation, it is further subjected to sonication and washing steps resulting in the formation of HA-Cys-CNGs. Anticancer drugs can be loaded into nanogels either by the means of physical adsorption or diffusion. 400 µg DOX is added to 5mg of HA-CNGs and HA-Cys-CNGs by incubating DOX under stirring for 24 hrs enabling drug adsorption and loading.

(b) Characterization of composite nanogels

Size distribution of the different composite nanogels preparations (DOX-HA-CNGs and DOX-HA-Cys-CNGs) were analyzed by Dynamic Light Scattering (DLS using Zetasizer, Malvern Instruments, USA). Size and surface morphology of the nanogels were further confirmed by using SEM (JEOL-JSM–6490 LA). The stability of composite nanogels suspension was determined by calculating surface charge obtained via zeta potential measurements (ZP- Zetasizer, Malvern Instruments, USA). FTIR spectra were recorded to determine the chemical structure of nanogels based on the bonding vibrations on Perkin-Elmer spectrum RXI. Thermal degradation studies were performed to determine the thermo-responsive properties of modified composite nanogels with varying temperature from 25^{o}C to 500^{o}C at a heating rate of 20^{o}C/min. Thermal history of control Chitin, Hyaluronic acid, control composite nanogels and drug loaded nanogels was studied through thermogravimetry and differential thermal analysis (TG/DTA) using (SII TG/DTA 6200 EXSTAR). Energy Dispersive X-ray (EDAX) (JEOL-JSM – 6490 LA) is used to determine the presence of sulphur in Cystamine. The scanning energy for EDAX analysis was done with 15 KeV with an elapsed time of 100 sec. In FT Raman, when a beam of laser focused on the sample, involving the scattered photons exchange energy with vibrational energy. By analyzing these vibrative motions in the molecules were obtained and determined. FT-Raman were performed using 1064 Nd:YAG laser BRUKER RFS 27: Stand alone FT-Raman Spectrometer to determine the characteristic peak of specific compounds with a spectral range of 50-4000cm^{-1} and a resolution of 2cm^{-1}.

(c) Rheological measurements

Rheological measurements were performed using Rheometer Kinexus Pro, USA, to find the visco-elastic property and

interaction between the constituting polymers. Rheological measurements were performed using dynamic oscillatory mode to determine elastic and viscous modulus as a function of frequency to calculate linear visco-elastic region (LVER) of nanogels. Measurements were performed with cone-plate geometry, for low viscosity nanogels 40mm upper cone and flat bottom plate geometry are used. Initially the sample is loaded onto the plate and performed the gap between the nanogel and plate which are calculated by force exerted by geometry. For low viscosity fluids like nanogels were performed with varying angular frequency from 0.1 to 10Hz. As a change in function of frequency elastic modulus (G'), viscous modulus (G'') and phase angle (δ) were calculated. Here the samples were studied under a constant temperature which are maintained by peltier apparatus is fixed to the instrument.[25]

(d) Hemolysis assay

The release of iron-containing protein hemoglobin into plasma causes hemolysis which can be determined by the means of damaged red blood cells.[38, 39] This study is performed to evaluate the hemocompatibility of the drug loaded composite nanogels. Hemolysis can be analyzed based on soret band based absorption of free hemoglobin at 415nm in blood plasma. Different concentrations of composite nanogels both control as well as drug loaded nanogels were taken for hemolytic assay (250, 500, 750 and 1000 µg/ml) of each of these samples, 100µL was treated with 1ml of blood and incubated for 2hr at 37°C in shaking incubator chamber. Saline and Triton x100 were used as positive and negative control for the samples. The absorbance was measured spectrometrically (BioTek Power Wave XS well plate reader) at 380nm, 415nm and 450 nm. The plasma hemoglobin can be calculated using the following equation. This procedure was performed as per earlier reported literature and calculated hemoglobin using the following equation. If the sample exceeds hemolysis value of 5% then it was considered to be hemolytic.[36,40]

Amount of Plasma Hb (mg/dL) = {(2A415) - [A380 + A450] x 76.25}

(e) Plasma Coagulation Study

Interaction of the composite nanogels with the plasma coagulation factors were analyzed by measuring coagulation time.[61] Platelet poor plasma (PPP) was separated from peripheral blood by centrifugation at 4000 rpm for 15 min. The prepared concentrations ranging from 250-1000 µg/ml of 50µL were added to 450µL of platelet poor plasma and kept in shaking incubator for 30 minutes at 37°C. After incubation, 50µL was taken from the above solution with pretreated composite nanogels was further added to 100µL of prothrombin reagent (Diagnostica stago, France) and the time is calculated for the plasma to coagulate i.e., prothrombin time (PT) was measured. In case of activated partial thromboplastin time (aPTT) measurements, 50 µL of aPTT activator (Diagnostica Stago, France) was added to 50 µL of plasma and incubated for 180 sec before the addition of 50µL of 0.025M $CaCl_2$. After $CaCl_2$ treatment, the time taken by plasma to coagulate was measured as aPTT. The values of PTT and aPTT are ratio values expressed in seconds. The experiments were performed in triplet and saline containing PPP were used as negative controls. [36,40]

(f) **In-vitro drug release**

Encapsulation efficiency can be calculated by means of standard curve drawn with known concentrations of doxorubicin (80, 70, 60, 50, 40, 30, 20, 10, 5ug/mL) to their corresponding OD values were noted. 40mg of composite nanogels (HA-CNGs and HA-Cys-CNGs) was loaded with 200uL of DOX (2mg/ml) and incubated for 24 hr under stirring. Furthermore, drug loaded composite nanogels were centrifuged at a rate of 20000rpm for 20min. The supernatant with the un entrapped DOX was measured using UV-Visible spectrophotometer (Shimadzu UV-Vis 1700) and drug concentration was calculated with respect to linear equation of standard curve.

In vitro release of DOX from HA-Cys-CNG composite nanogels were studied using eppendorf method. 500uL of DOX-HA-Cys-CNGs dispersed in PBS (pH 7.4) were added to different eppendorf tubes and the released DOX at different time interval was quantified by centrifuging each eppendorfs and analyzing the supernatant spectrophotometrically. Two set of experiments were carried out in the absence and presence of GSH (10mM).
% DOX released = (Amount of DOX present in the supernatant/ Initial amount of DOX entrapped within the nanogel)

(g) Cell Culture

HT-29 and IEC-6 were maintained in Dulbecco's modified Eagles Medium (DMEM) supplemented with 10% fetal bovine serum (FBS). The cells were incubated in 5% CO2 incubator. After reaching confluence, the cells were detached from the flask with Trypsin-EDTA. The cell suspension was centrifuged at 3000 rpm for 3 min and then resuspended in the growth medium for further study.

(h) Cell uptake studies by fluorescent microscopy

Acid etched cover slips kept in 12 well plates were loaded with HT-29 and IEC-6 cells with a seeding density of 20,000 cells per cover slip and incubated for 24 h for the cells to attach to the well. After 24 h incubation, the medium was removed and the wells were carefully washed with PBS buffer. Then, the nanogel preparations, at a concentration of 0.25 mg/mL were added along with the media in triplicate to the wells and incubated for a time period of 12 h. After the incubation time, media with sample were removed and the cover slips were processed for fluorescent microscopy. The processing involved washing the cover slips with PBS and fixing the cells in 3.7% Para formaldehyde (PFA) followed by a final PBS wash. The cover slips were air dried and mounted on to glass slides using DPX. The slides were then

viewed under the fluorescent microscope (Olympus-BX-51) to understand the localization of doxorubicin loaded composite nanogels at different depth of dermal penetration.

(i) Cell uptake studies by flow cytometry

Flow cytometry techniques were used to quantify the intra cellular fluorescence of DOX within both normal (IEC-6) and colon cancer (HT-29) cells. The cells were seeded at a density of 50,000cells/well. Followed by cell attachment DOX-HA-CNGs, DOX-HA-Cys-CNGs and DOX-CNGs were added and incubated for 12 hours. After the incubation time, cells were washed, trypsinised and later quantified the fluorescence intensity using the flow cytometer with excitation at 488 nm argon laser using FACS Aria II (Beckton and Dickinson, Sanjose, CA) and measuring the emission at 520nm. A minimum of 10,000 events per sample was analyzed.

(j) Cytotoxicity studies

Cell cytotoxicity (MTT) assay was performed to determine the percentage of viable cells which reduced the tetrazolium component into purpled colored formazan crystals. For cytotoxicity studies, 10,000 cells/well were seeded on a 96 well plate and after 24 h, cells were treated with different concentrations of DOX-HA-CNGs and DOX-HA-Cys-CNGs diluted in media. Along with this, the same concentrations of DOX-HA-Cys-CNGs were diluted in media containing 10 mM GSH to the cells seeded in the 96 well plates. After 48 hrs, media was removed and MTT assay was performed as per the literature.[21] Using Elisa micro plate reader optical densities were measured at a wavelength of 570nm.

(k) Statistical analysis

The experiments were carried out in triplicates and values are expressed as mean ± standard deviation (SD). A Student's t-test was conducted to determine the significance. A probability level of $p < 0.05$ was considered to be statistically significant.

Results and discussion

HA-Chitin composite nanogels were successfully synthesized by an ionic interaction between the carboxyl groups of HA and hydroxyl group of chitin. Cystamine was conjugated using EDC/NHS conjugation chemistry. So here EDC activated carboxyl group of HA interacts with amine group at one end of cystamine through amide bond and the unreacted amine group forms ionic interaction with hydroxyl group of chitin resulting in a cross linked nanogel system. Fig. 1 represents the hypothetical reaction scheme showing the interaction of these components. Within a cancer cell GSH will cleave the disulphide bond in the cross-linked cystamine thereby releasing out the loaded therapeutic agent.[32]

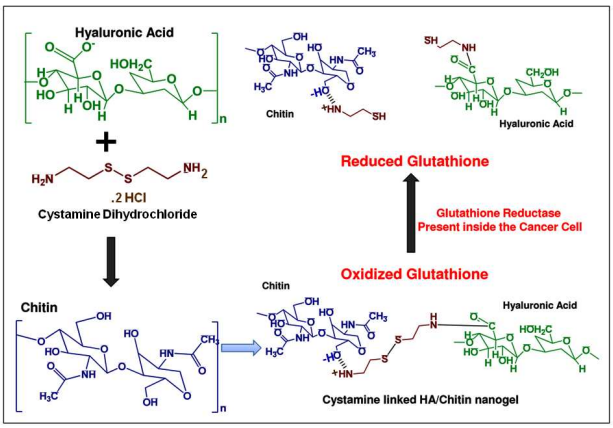

Fig.1. Reaction scheme of composite HA-Cys-CNGs formation showing the interaction between HA, Chitin and cystamine.

Anticancer agent, DOX was loaded into these composite nanogels following an overnight interaction under stirring. During the reaction time, DOX will be physically entrapped into the cross linked nanogel mesh as well as physically adsorb on to the nanogels. DOX-HA-Cys-CNGs were further washed thrice to remove the unbound and unreacted components.

Table 1 shows the size distribution of composite nanogels, both DOX-HA-CNGs and DOX-HA-Cys-CNGs analyzed using DLS. The synthesis technique resulted in 100±20nm sized DOX-HA-CNGs and 160±35nm DOX-HA-Cys-CNGs. Cystamine conjugation has increased the size of the composite nanogels which shows the presence of the new moiety cystamine. The zeta potential of +30mV and +24mV for DOX-HA-CNGs and DOX-HA-Cys-CNGs indicated the positive surface charge and stability.

There was a size increment for these nanogels from 160nm to 265 nm after dispersing in media. This could be due to the aggregation caused by protein binding. But in the preclinical scenario, these targeted nanogels will be reaching the tumor site within a short time. So even if there might be some aggregation followed by clearance these nanosized formulation will enhance the availability of the chemotherapeutic agent at the tumor site.

Samples	Size	PDI
DOX-HA-CNGS	100±20 nm	0.293
HA-Cys-CNGs	160±45 nm	0.258
DOX-HA-Cys-CNGs	120±25 nm	0.251
HA-Cys-CNGs in cell culture media	265±35 nm	0.243

Table. 1 Size distribution by DLS of DOX-HA-CNGs and DOX-HA-Cys-CNGs composite nanogels

SEM images (Fig.2) of these composite nanogels correlated well with the DLS result indicating spherical morphologies (but slightly interlinked and agglomerated since nanogels) within 200 nm size range showed black spots which could be due to the water based nanogels and over drying of sample and showed

spherical particles. Cystamine-composite nanogels also showed spherical particles which could be due to the cross linking of cystamine between hyaluronic acid and chitin to form nanogels. The polydispersive index (PDI) of these composite nanogels was less than 0.3 representing the size parameters are monodispersed. These composite nanogels can be used as drug delivery vehicles.

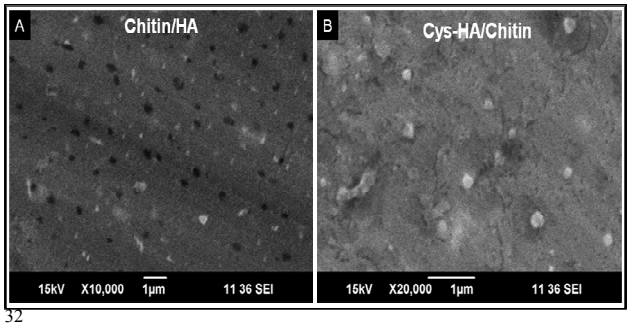

Fig.2 SEM images of DOX-HA-CNGs (A) and DOX-HA-Cys-CNGs (B).

Furthermore to determine the presence of disulphide bond between chitin and hyaluronic acid, FT Raman was used. Fig 3 could be explained the cystamine by indicating the presence of disulphide group in the spectral region around 510cm^{-1}.[41–44] The peak of the disulphide were very sharp but with a low intensity which is due to the very less concentration added in composite nanogels.

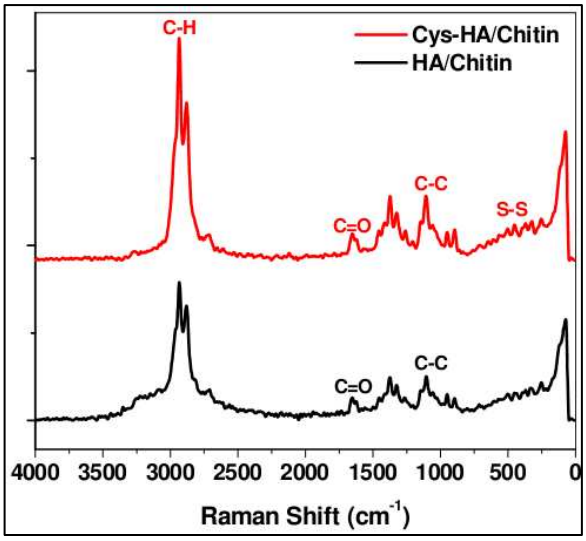

Fig.3. FT Raman spectrum composite nanogels of HA/chitin (a) and Cys-HA/Chitin (b)

FT-IR were performed to find the interaction and bonding of composite nanogels between polymers and also to confirm the presence of drug loaded in composite nanogels. From the IR spectrums (Fig. 4) shows a peak at 1630cm^{-1} which corresponds to the strong absorption band of N-H stretch of chitin. In HA, the strong bands at 3450cm^{-1} can be attributed to O-H band, 1674cm^{-1} and 1536cm^{-1} can be attributed asymmetric bending (C=O) and symmetric bending (C-O) of carboxyl group respectively. The aliphatic stretches (C-H) are at 2900cm^{-1} and 1450-1500cm^{-1} corresponding to SP orbital stretches of HA were shown. Upon blending of HA with chitin, there is possibility that there amide linkage is formed between chitin and HA in $CaCl_2$ methanol solvent, that could be attributed from absorption bands at about 1653.21cm^{-1} and 1563.68cm^{-1} of amide I and II bands respectively.[36] The characteristic peaks of Doxorubicin are of C=C stretch at 1570 cm^{-1}, =CH stretch at 3610cm^{-1}, which is overlapped with hydroxyl group peak around 3600 cm^{-1}. These peaks could be seen in the sample nanogels. The characteristics peaks of C-S stretch around 670cm^{-1} in cystamine conjugated composite nanogels and whereas in control composite nanogels these peaks were not seen clearly. The C-S stretch peak is of weak signal, so as to further confirm cystamine presence in composite nanogels, FT-Raman was performed.[45]

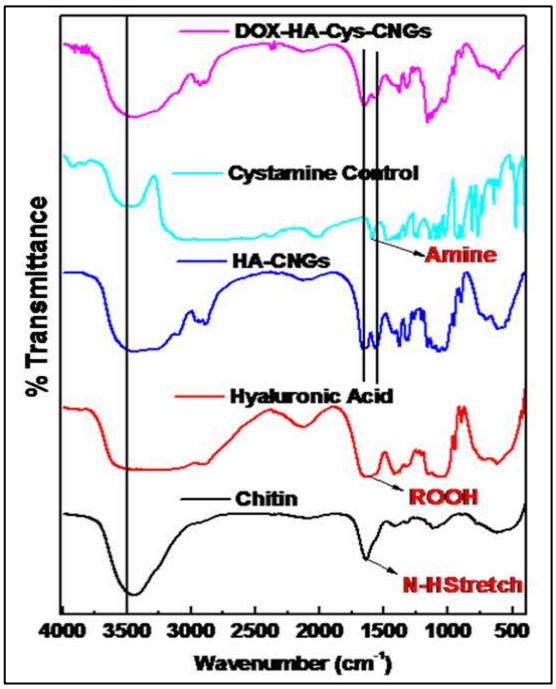

Fig.4. FT-IR spectroscopy of composite nanogels α-chitin (a), Hyaluronic acid (b), Dox control (c), Control cystamine (d), Control HA/Chitin composite (e), Drug loaded HA/chitin composite nanogels (f), Cys-HA/Chitin composite nanogels(g), Cys-HA/Chitin composite nanogels (h)

Fig 5 shows the TGA (left) and DTG (right) curve for composite nanogels. In Fig.5 (A) from the TGA profile the first step of degradation of nanogels at less than 100°C has a minimum of 8% of degradation which is due to the presence of moisture and water content in the compound. 15% of Degradation of hyaluronic acid at the same temperature proves the water retention property of HA.[46] The composite nanogels showed two step degradation at a temperature 250°C and 343°C. HA/Chitin nanogels were degraded with two step degradation of 50% weight loss at temperatures 250°C. The weight losses were very slow and

gradual degradation at 400°C when cystamine were conjugated with HA/Chitin nanogels. The weight losses of Cys-Ha/Chitin nanogels were comparatively lower when compared to HA/Chitin nanogels at a temperature from 290°C to 240°C. First step of degradation occur due to the presence decomposition low molecular weight compounds like polysaccharides structure in composite nanogels. When the temperature increases at range of 400°C the main backbone structure was degraded with a heavy weight loss.[47]

Differential thermal gravimeter (DTG) was performed to understand the behavior of cystamine conjugated composite nanogels with control composite nanogels. As temperature varies the affinity for water when solid state macromolecules which could have disordered structure that can be easily hydrated. First order differentiation of TGA is DTG, this explains the mechanism of the material whether it is endothermic or exothermic, where polysaccharides would have hydration properties depending on varying molecular structures in the nanoformulations. Thus the control composite nanogels and cystamine conjugated composite nanogels showed a different water holding capacity this could be due to the effect of amorphous nature in the nanoformulations (**Fig.5 (B)**). Corresponding to the TGA the endothermic and exothermic peaks are interpreted in DTG and this shows that the exact degradation point in thermal degradation. [48,49]

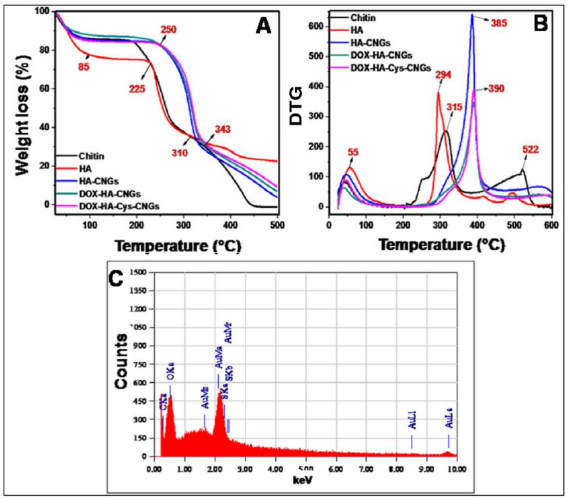

Fig.5. TG thermograms (A), DTG (B) for Chitin, HA, HA-CNGs, DOX-HA-CNGs and DOX-HA-Cys-CNGs, EDAX (c) plot of HA-Cys-CNG composite nanogel.

To determine the presence of cystamine in the composite nanogels, EDAX analyses were performed. This study confirms the presence of sulphur in sample with a very less mass percentage of 0.98%, where the amounts of cystamine added to the composite nanogels were also comparatively same to the EDAX value in **Fig. 5(C).** In this most dominant compounds present are carbon with mass value 53% and sputter coated with gold were showed a higher value of 45%.

From **Fig.6** elastic modulus (G'), viscous modulus (G") and phase angle (δ) were measure as a function of frequency from 0.1 to 10Hz. Elastic modulus is independent to that of the frequency till 2Hz and there is a slight deviation as a function of frequency. But viscous modulus is completely independent to that of the frequency until frequency 1Hz and the values of viscous modulus increases and completely dependent to that of frequency which is more than 1Hz. Here the this represents that the loss modulus is higher and when once the nanogels are start swelling and it would not regains its energy and more swelling nature of nanogels until the whole structure is deformed and degraded completely. This can be further confirmed with phase angle of nanogels, here at initial frequency the phase angle is very minimal around 15° and when it reaches the 1Hz the value of phase angle changed drastically to 50°. With this the stability of the composite nanogels are nearly same for both the control Chitin/HA and Cys-HA/Chitin composite nanogels.[50,51]

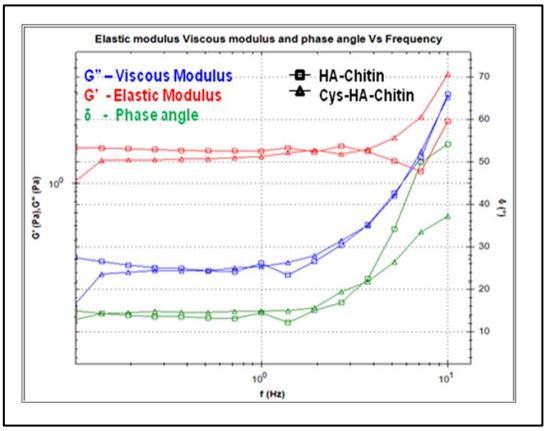

Fig.6. Rheological measurement of HA-CNG nanogels and HA-Cys-CNGs

Hemolysis study was evaluated for the nanogel systems and the results showed that the hemolytic ratio of samples varying from 250µg/mL to 1mg/mL is less than 5% of hemolysis in RBC cells. These results showed that the nanoformulations are safe for IV administration. (**Fig. 7**).

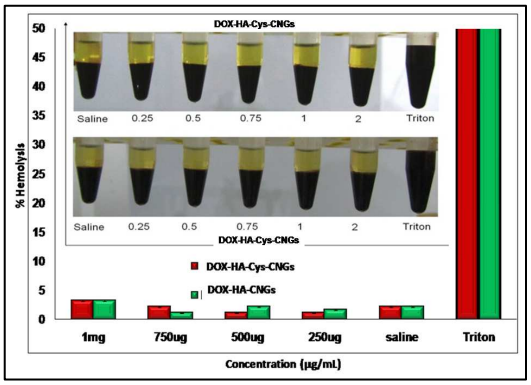

Fig.7. Hemolysis assay of DOX-HA-CNGs and DOX-HA-Cys-CNG composite nanogels

To find the effect of these nanoformulations on plasma coagulation, PT/aPTT study was performed. Different concentration of samples were taken from 250-2000µg/mL and treated with platelet poor plasma and coagulation time is measured. The normal range of prothrombin time falls from 12-15sec and aPTT values falls in 27-35sec. The PT/aPTT values of both DOX-HA-CNGs and DOX-HA-Cys-CNGs lies in the normal range (Table.2) indicating that the composite nanogels have no effect on the intrinsic and extrinsic coagulation pathway. Thus PT and aPTT measurements proved that the nanoformulations do not interact with the coagulation factor proteins, thereby causing no interference with the plasma coagulation study.

Dox-HA/Chitin			Dox-Cys-HA/Chitin		
Concentration (µg/mL)	PT (sec)	aPTT (sec)	Concentration (µg/mL)	PT (sec)	aPTT (sec)
250	15.0	33.4	250	14.5	32.95
500	15.0	31.75	500	14.6	32.0
750	14.9	32.2	750	14.4	32.25
1000	14.8	33.3	1000	14.7	33.45
2000	14.7	31.75	2000	14.4	31.8

Table.2. PT and aPTT values of DOX-HA-CNGs and DOX-HA-Cys-CNGs composite nanogels

The loading efficiency is calculated with different incubation timing with same composite nanogels. Doxorubicin is highly hydrophilic, this prevented from the loading the drug into the polymeric nanoregime matrix. Since the complete system is based on water easily the drug comes out from both control and conjugated nanogels. The loading efficiency was not more than 30%, when there is an increase in incubation time from 12 to 24 hr the drug loaded were maximum to 33%. Most of the drug would easily come out when a high centrifugation is given to the samples. Similarly, cystamine conjugated nanogels were also found to be the same as the control composite nanogels.

In vitro drug release of DOX from the composite nanogels was performed at pH 7.4 in the presence and absence of GSH (Fig. 8). Around 32 % of DOX was released from DOX-HA-Cys-CNGs whereas the presence of 10 mM GSH enhanced the release to 53% within 6 hrs. Even though this could be considered as a burst release there was a significant impact of GSH on the DOX release. Later on there was very slow releases of DOX till 48hr. For about 2 days there was a sustained release of DOX from the composite nanogels resulting in a significant difference in the percentage of DOX released due to the presence of GSH. This proves the sensitiveness of DOX-HA-Cys-CNGs towards GSH environment. The cancer cells are reported to have 10mM GSH which would cause an enhanced intracellular release of DOX enabling improved cancer cell death.[3]

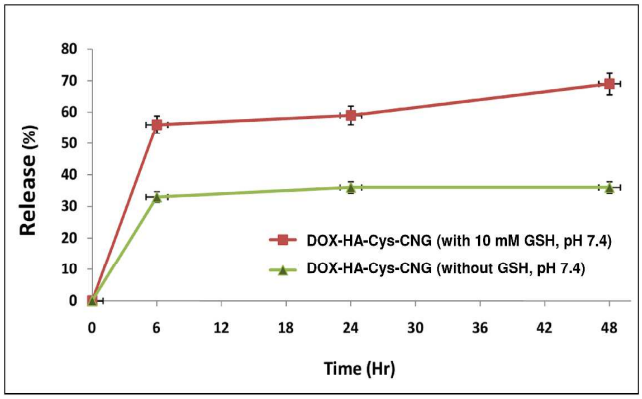

Fig.8. In vitro release in 7.4pH of both drug loaded cystamine conjugated nanogels with 10mM GSH (Red Square) and without GSH (Green triangle)

Intracellular localization and the cancer cell targetability of the nanogel preparations were demonstrated quantitatively by fluorescent microscope (Fig.9) and qualitatively by flow cytometry (Fig.10). Since the doxorubicin has an inherent fluorescence it can directly emit a red colour which can be used for analysis.

To confirm the localization of the nanogels within the intracellular compartments, fluorescent intensities of DOX from the nanogel preparations were tracked, analyzed and photographed. Fig. 9 represents the fluorescent microscopic images of HT-29 cells and IEC-6 cells treated with DOX-CNGs, DOX-HA-Cys-CNGs and the control cells. Here we can observe an enhanced intensity of DOX within the HT-29 cells treated with DOX-HA-Cys-CNGs compared to that of DOX-CNGs. This could be due to the fact that HA posses an affinity towards CD 44 receptors expressed by the cancer cells. Comparing CD-44 +ve HT-29 and CD44–ve IEC-6 cells, there is a clear enhanced internalization within HT-29 cells proving HA target ability towards CD44. [29]

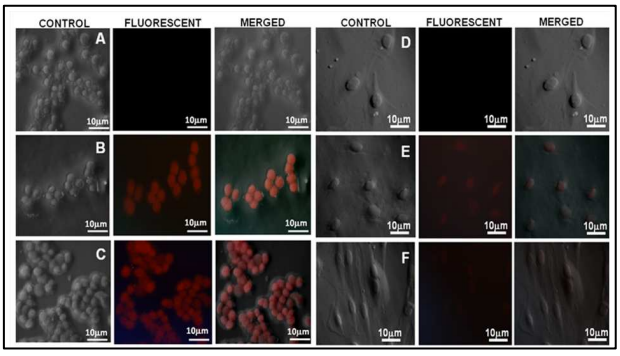

Fig. 9. Fluorescent microscopic images of HT-29 cells IEC-6 cells. Control cells (A), cells treated with DOX-CNGs (B), DOX-HA-Cys-CNGs for 12 hr.

Cellular uptake of the nanogel preparations were quantitatively analysed by flow cytometry. Fig.10 represents the histograms obtained from the flow cytometric analysis of HT-29 and IEC-6 cells treated with DOX-CNGs, DOX-HA-CNGs and DOX-HA-Cys-CNGs. Around 31% of HT-29 cells showed uptake of DOX-CNGs whereas around 81 and 86% cells had taken up HA incorporated nanogels. IEC-6 cells comparatively showed lesser uptake where the HA incorporation reduced the uptake of DOX-CNGs from 23% to 6 and 10%. The result supported the fact that HA complexation aids in enhancing the cellular uptake by CD44 +ve cancer cells.

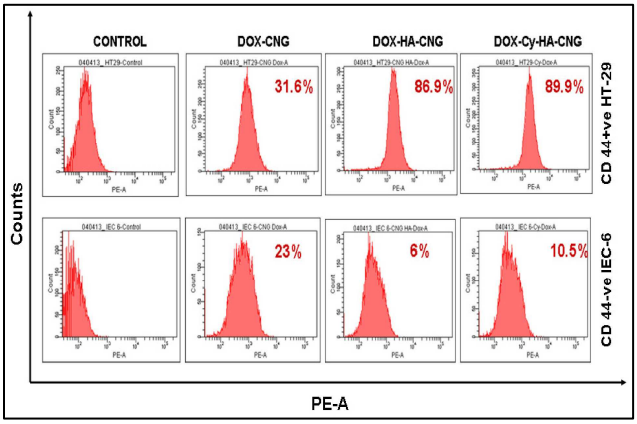

Fig.10. Flowcytometric analysis of cellular uptake of nanogel preparation by CD44+ve cancer cell (HT-29) and CD44–ve normal cells (IEC-6) after 12hr incubation

MTT assay were carried out to find out the toxicity induced by DOX-CNGs, DOX-HA-Cys-CNGs and DOX-HA-Cys-CNGs (with GSH) towards IEC-6 and HT-29 cell lines. The potency of DOX towards cancer cells is well established as DOX interchelates with DNA and inhibits the biosynthesis of macromolecules and also the progression of Topoisomerase II, which prevents from replication by means of DNA binding mechanism. The cell viability profile for HT-29 cells (Fig.11A) shows that there is a significant enhancement in the toxicity induced by DOX-HA-Cys-CNGs and DOX-HA-Cys-CNGs (with GSH) compared to that of DOX-CNGs to CD44+ve HT-29 cells. Even though these composite nanogels are inducing toxicity towards CD44-ve IEC-6 cells (Fig.11B), there is no statistical significance in comparing the groups. So the study shows that HA aided CD- 44 mediated uptake of these nanogels and the intracellular GSH within HT-29 cells might have reduced the disulphide bond releasing more DOX thereby inducing more toxicity. Also in the case of DOX-HA-Cys-CNGs (with GSH) the presence of GSH in the media itself caused –S-S- bond cleavage enhancing more amount of DOX casing significantly enhanced cancer cell death. This is not happening within CD 44 –ve IEC-6 cells. The cells carry out normal endocytosis of the nanosized moieties and the potent DOX caused the cell death. Thus the study clearly shows that HA enhanced the targeted delivery of DOX towards CD44+ve HT-29 compared to that of CD44-ve IEC-6 cells.

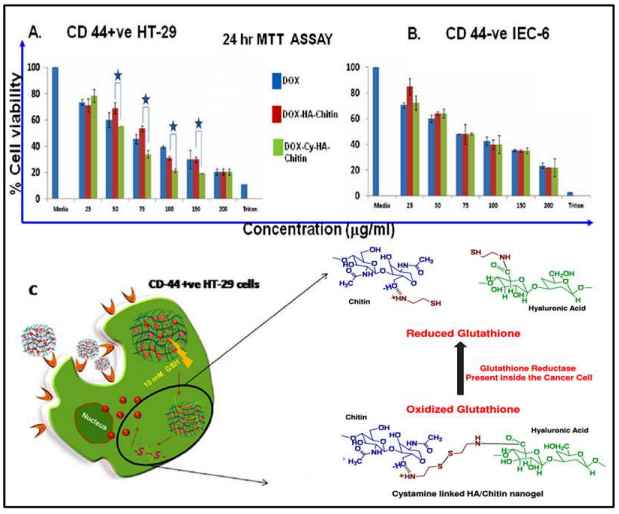

Fig. 11. Cell viability profile of HT-29 (A) and IEC-6 (B) cells treated with DOX loaded composite nanogels for 24 hr analyzed by MTT assay. Representative hypothetical scheme of mechanism of toxicity induced in a CD 44+ve HT-29 cancer cell (C). * and # represents the statistical significance between the DOX-CNG and DOX-HA-Cys-CNG along with DOX-CNG and DOX-HA-Cys-CNG

Conclusions

In summary, we have developed composite nanogels based on chitin and hyaluronic acid. Cystamine was conjugated HA-Chitin composite nanogels and loaded with anticancer agent doxorubicin. These composite nanogel preparations were characterized by DLS, SEM, FTIR, and rheological parameters. The nanogels within 200 nm size range showed redox responsive behavior in presence of GSH. Flow cytometric quantitative analysis and fluorescent microscopic qualitative analysis proved selective uptake of DOX-HA-CNGs by CD 44 +ve colon cancer cells (HT-29) in comparison to that of CD-44 –ve normal epithelial cells (IEC-6). HA incorporation aided in CD-44 targeting of these nanogels to HT-29 colon cancer cells thereby inducing redox responsive and enhanced cancer cell death. Thus this redox responsive CD-44 specific nanogel system could be used as a better drug delivery agent for the targeted intracellular delivery of therapeutic agents for efficient cancer treatment.

Acknowledgements:

The authors acknowledge The Department of Biotechnology (DBT), Government of India supported this work under a Nanoscience and Nanotechnology Initiative program (Ref. No. BT/PR10850/NNT/28/127/2008) for providing financial support. Author **S. Maya** is thankful to Council of Scientific and Industrial Research (CSIR), India for providing Senior Research Fellowship (SRF Award No.: 9/963 (0012) 2K11-EMR-I).

Notes and References

[#]Authors contributed equally.
Amrita Centre for Nanosciences and Molecular Medicine, Amrita Institute of Medical Sciences and Research Centre, Amrita Vishwa Vidyapeetham University, Kochi-682041, India.
*Corresponding author: E-mail ID: rjayakumar@aims.amrita.edu & jayakumar77@yahoo.com (Prof. R. Jayakumar)
Tel.: +91 484 2801234 Fax: +91 484 2802020.

[1] J. Cheon, J.H. Lee, Acc. Chem. Res., 2008, 41, 1630.
[2] S. Seo, C.S. Lee, Y.S. Jung, K. Na, Carbohydr. Polym., 2012, 87, 1105.
[3] Y.J. Pan, Y.Y. Chen, D.R. Wang, C. Wei, J. Guo, D.-R. Lu, C.-C. Chu, C.-C. Wang, Biomaterials, 2012, 33, 6570.
[4] S. Nair, N.S. Remya, S. Remya, P.D. Nair, Carbohydr. Polym., 2011, 85, 838.
[5] K.L. Spiller, Y. Liu, J.L. Holloway, S.A. Maher, Y. Cao, W. Liu, G. Zhou, A.M. Lowman, J. Control. Release., 2012, 157, 39.
[6] M. Hamidi, A. Azadi, P. Rafiei, Adv. Drug Deliv. Rev., 2008, 60, 1638.
[7] M. Bindusri, V. Ashok, A. Chattergy, Int. J. Pharm. Chem. Sci. 2012, 1, 642.
[8] S.J. Kim, S.J. Park, S.I. Kim, Reac. Func. Pol., 2003, 55, 53.
[9] W. E. Hennink, C.F. van Nostrum, Adv. Drug Deliv. Rev., 2012, 64, 223.
[10] Y. Jiang, J. Chen, C. Deng, E.J. Suuronen, Z. Zhong, Biomaterials, 2014, 35, 18, 4969.
[11] J.K. Oh, R. Drumright, D.J. Siegwart, K. Matyjaszewski, Prog. Polym. Sci., 2008, 33, 448.
[12] M.M. Yallapu, M. Jaggi, S.C. Chauhan, Drug Discov. Today, 2011, 16, 457.
[13] S. Shidhaye, V. Lotlikar, S. Malke, V. Kadam, Curr. Drug Therapy, 2008, 3, 209.
[14] L. Messager, N. Portecop, E. Hachet, V. Lapeyre, I. Pignot-Paintrand, B. Catargi, R. Auzély-Velty, V. Ravaine, J. Mater. Chem. B., 2013, 1, 3369.
[15] J.H. Ryu, R.T. Chacko, S. Jiwpanich, S. Bickerton, R.P. Babu, S. Thayumanavan, J. Am. Chem. Soc., 2010, 132, 17227.
[16] K.Y. Choi, K.H. Min, H.Y. Yoon, K. Kim, J.H. Park, I. C. Kwon, K. Choi, S.Y. Jeong, Biomaterials, 2011, 32, 1880.
[17] K.Y. Choi, G. Saravanakumar, J.H. Park, K. Park, Colloids Surf. B. Biointerf., 2012, 99, 82.
[18] E. Garcia-Garcia, K. Andrieux, S. Gil, P. Couvreur, Int. J. Pharm., 2005, 298, 274.
[19] Y. Kim, M. Thapa, D.H. Hua, K.O. Chang, Antiviral Res., 2011, 89, 165.
[20] F. Brunel, L. Véron, C. Ladavière, L. David, A. Domard, T. Delair, Langmuir, 2009, 25, 8935.
[21] H. Qian, X. Wang, K. Yuan, C. Xie, W. Wu, X. Jiang, L. Hu, Biomater. Sci., 2014, 2, 220.
[22] N.S. Rejinold, R. Biswas, G. Chellan, R. Jayakumar, Int. J. Biol. Macromol., 2014, 67, 279.
[23] H. Asadi, K. Rostamizadeh, D. Salari, M. Hamidi, Int. J. Pharm., 2011, 416, 356.
[24] R.D. Price, M.G. Berry, H. Navsaria, J. Plast. Reconstr. Aesthet. Surg., 2007, 60, 1110.
[25] C.E. Schanté, G. Zuber, C. Herlin, T.F. Vandamme, Carbohydr. Polym., 2011, 85, 469.
[26] N. Goodarzi, M.H. Ghahremani, R. Dinarvand, J. Med. Hypotheses. Ideas, 2011, 1.
[27] J. Necas, L. Bartosikova, P. Brauner, J. Kolar, Vete. Med. , 53, 397.
[28] K. Young, G. Saravanakumar, J. Hyung, K. Park, Colloids Surfaces B Biointerfaces, 2012, 99, 82.
[29] K. Chen, F. Pan, H. Jiang, J. Chen, L. Pei, F. Xie, H. Liang, Clin. Exp. Metastasis, 2011, 28, 751.
[30] B. Delpech, N. Girard, P. Bertrand, M. N. Courel, C. Chauzy, Delpech, J. Intern. Med., 1997, 242, 41.
[31] H. Tamura, T. Furuike, S. V. Nair, R. Jayakumar, Carbohydr. Polym., 2011, 84, 820.
[32] R. Cheng, F. Feng, F. Meng, C. Deng, J. Feijen, Z. Zhong, J. Control. Release, 2011, 152, 2.
[33] L.V Christensen, C.W. Chang, W.J. Kim, S.W. Kim, Z. Zhong, C. Lin, J.F.J. Engbersen, J. Feijen, Bioconjug. Chem., 2006, 17, 1233.
[34] N. Rapoport, W.G. Pitt, H. Sun, J.L. Nelson, J. Control. Release, 2003, 91, 85.
[35] N.S. Rejinold, A. Nair, M. Sabitha, K.P. Chennazhi, H. Tamura, S.V. Nair, R. Jayakumar, Carbohydr. Polym., 2012, 87, 943.
[36] A.L. Daniel-da-Silva, L. Ferreira, A.M. Gil, T. Trindade, J. Colloid Interface Sci., 2011, 355, 512.
[37] M. Sabitha, N. Sanoj Rejinold, A. Nair, V.K. Lakshmanan, S.V Nair, R. Jayakumar, Carbohydr. Polym., 2013, 91, 48.
[38] R. Jayakumar, A. Nair, N.S. Rejinold, S. Maya, S.V. Nair, , Carbohydr. Polym., 2011, 87, 2352.
[39] T. R. Arunraj, N. Sanoj Rejinold, N. Ashwin Kumar, R. Jayakumar, Int. J. Biol. Macromol., 2013, 62, 35.
[40] J.M. Koziara, J.J. Oh, W.S. Akers, S.P. Ferraris, R.J. Mumper, Pharm. Res., 2005, 22, 1821.
[41] A. Torreggiani, A. Tinti, Metallomics, 2010, 2, 246.
[42] H. Katas, N.N. S. Nik Dzulkefli, S. Sahudin, J. Nanomater., 2012, 2012, 1.
[43] A. Kudelski, W. Hill, Langmuir, 1999,15, 3162.
[44] S. Gunasekaran, E. Sailatha, S. Seshadri, S. Kumaresan, Indian J. Pure & Appl. Phys., 47, 2009,12.
[45] P. Nigam, S. Waghmode, M. Louis, S. Wangnoo, P. Chavan, D. Sarkar, J. Mater. Chem. B, 2014, 2, 3190.
[46] A.Anitha, U. Saji, S.V Nair, R.Jayakumar, V.K. Lakshmanan, , J. Biomed. Nanotechnol., 2012, 9, 1.
[47] S. Ramesh, R. Shanti, E. Morris, Carbohydr. Polym., 2013, 91, 14.
[48] M.C.I. Mohd Amin, N. Ahmad, N. Halib, I. Ahmad, Carbohydr. Polym., 2012, 88, 465.
[49] E. Chornet, D. Rodrigue, Carbohydr. Polym., 2007, 67, 586.
[50] H. Jiang, W. Su, P.T. Mather, T.J. Bunning, Polymer, 1999, 40, 4593.
[51] A. Taki, B. John, S. Arakawa, M. Okamoto, Eur. Polym. J., 2013, 49, 923.
[52] E. Ye, P. L. Chee, A. Prasad, X. Fang, C. Owh, V. J. J. Yeo, X. J. Loh, Mater. Today, 2014, 17, 194.